

Article

The Use of Tailings to Make Glass as an Alternative for Sustainable Environmental Remediation: The Case of Osor, Catalonia, Spain

Pura Alfonso ¹, Oriol Tomasa ¹, Luis Miguel Domenech ^{2,3}, Maite Garcia-Valles ^{2,*}, Salvador Martinez ² and Núria Roca ⁴

¹ Departament d'Enginyeria Minera, Industrial i TIC, Universitat Politècnica de Catalunya Barcelona Tech, Av. de les Bases de Manresa 61–63, 08242 Manresa, Spain; maria.pura.alfonso@upc.edu (P.A.); oriol.tomasa@upc.edu (O.T.)

² Departament de Mineralogia, Petrologia i Geologia Aplicada, Universitat de Barcelona, Carrer Martí i Franquès 1, 08028 Barcelona, Spain; lmdomenech@ub.edu (L.M.D.); salvadormartinez@ub.edu (S.M.)

³ Departament de Mecànica de Fluids, Universitat Politècnica de Catalunya Barcelona Tech, Carrer Colom 11, 08222 Terrassa, Spain

⁴ Departament de Biologia Evolutiva, Ecologia i Ciències Ambientals, Universitat de Barcelona, Av. Diagonal 343, 08028 Barcelona, Spain; nroca@ub.edu

* Correspondence: maitegarciavalles@ub.edu; Tel.: +34-934-02-13-48

Received: 17 August 2020; Accepted: 14 September 2020; Published: 16 September 2020



Abstract: Tailings from the Osor fluorite mines release large amounts of potentially toxic elements into the environment. This work is a proposal to remove these waste materials and use them as a raw material in the manufacture of glass. The chemical composition of the tailings was determined by X-ray fluorescence and the mineralogy by X-ray diffraction. Waste materials have SiO₂, Al₂O₃ and CaO contents suitable for a glass production, but Na as NaCO₃ has to be added. Two glass formulations, with 80–90% of the residue and 10–20% Na₂CO₃, have been produced. The crystallization temperatures, obtained by differential thermal analysis, were 875 and 901 °C, and the melting temperatures were 1220 and 1215 °C for the G₈₀₋₂₀ and G₉₀₋₁₀ glasses, respectively. The transition temperatures of glass were 637 and 628 °C. The crystalline phases formed in the thermal treatment to produce devitrification were nepheline, plagioclase and diopside in the G₈₀₋₂₀ glass, and plagioclase and akermanite-gehlenite in the G₉₀₋₁₀ glass. The temperatures for the fixed viscosity points, the working temperatures and the coefficient of expansion were obtained. The chemical stability of the glass was tested and results indicate that the potentially toxic elements of the tailings were incorporated into the glass structure.

Keywords: recycling; tailings; glass; workability

1. Introduction

Tailings produce a large number of environmental impacts [1]. Especially dangerous are the problems that occur when the tailings result from the processing of sulphide ores. In these cases the interaction of meteoric water with the sulphides remaining in the tailings drives the generation of acid drainage, which can carry large amounts of potentially toxic elements [2–4]. These elements are liberated into the environment and produce pollution in water, which cannot be used for other applications. Special care must be taken in those tailings with small particles, since this enlarges the reactive surface, thus promoting the development of acid-generation reactions [5].

The world consumption of mineral resources is very large and produces a large amount of waste, which has been reported as at least 5 to 7 billion tons of mine tailings per year [6], and up to 14 billion

tons per year [7]. It is expected this will increase throughout the 21st century due to the need to exploit ores with lower grade [8]. Thus, management strategies that contribute new solutions for sustainable development need to be adopted. The recycling of these tailings is an attractive proposal for tailings management. This has a double benefit since the volume of new exploitations can be reduced, which is one of the principles of the circular economy [9]. On the other hand, materials from tailings frequently have high homogeneity and a fine particle size, which is useful for many applications and important energy savings can be obtained.

Moreover, the recycling of tailings for use as raw materials for the manufacture of glass and glass-ceramics removes the hazardous elements from the environment. Vitrification is a stabilization technology for hazardous wastes since it converts them into a stable glass or glass-ceramic that is suitable for manufacturing products for commercial purposes [10,11]. The mine wastes used in glass manufacturing have been extensively studied to produce glass [12–14], glass fibres [15] and glass-ceramics [16–19].

In this work, the tailings from the Osor mines (Girona, Catalonia, Spain), are characterized and their viability to be used as raw material for the production of commercial glass is evaluated. This is a proposal for using these raw materials in the manufacture of glass, thus contributing to the remediation of the old mining area. The Osor tailings are of special interest for making glass. They show two favourable characteristics in their chemical composition because they are waste materials of an old mine in which one of the ores was fluorite; thus, these residues are rich in fluorine and calcium. These elements favour the manufacture of glass, so the addition of CaF_2 decreases melting and sintering temperatures [20]. CaF_2 can play an important role in the properties of glass and glass-ceramics [21,22]. Fluorine replaces bridging oxygens in the glass network by nonbridging fluorine, which disrupts and weakens the glass network [21]. Calcium can act as a network modifier and as charge compensator for the deficiency in positive charges produced by the Al-Si substitution in the tetrahedral sites [23,24] in silicate glasses, which depolymerizes the glass network following the formation of nonbridging oxygen.

The Osor mines became one of the most important mines in Catalonia, and were exploited from Roman times until the 1980s. The volume of production was especially high between 1942 and 1980, with a daily production during the last period of activity of 80 to 90 tons of fluorite, 10 to 12 tons of zinc, and 6 to 7 tons of lead [25]. Although the mine water has a neutral pH due to the high content of neutralising minerals, it is rich in metals, especially Cd, Co, Pb, Zn, As, Ba and Sb [26], leached from the breakage of the sulphide minerals. Part of these pollutants come directly from the mine adits but also from the tailings. The small particle size of the tailings, less than 200 μm , contributes to the high pollution in soils, sediments and surface waters of the area. The tailings containing potentially toxic elements are leached and end up in the river that is a few meters from the dump [27,28].

2. Materials and Methods

2.1. Materials

The Osor mines are located in the Montseny massif, Prelitoral Catalan coastal range, 30 km west of the city of Girona. The mine exploited Ba-F-Pb-Zn veins hosted in metapelitic rocks of Paleozoic age. Such veins are abundant in the Catalonian coastal ranges with other exploited deposits, such as the Berta mine [29]. The exploited minerals were mainly fluorite, galena and sphalerite, hosted in quartz, with a minor amount of calcite, barite and pyrite.

The tailings sample used in the present study came from the flotation process in the mineral processing plant of Osor, Girona, Spain (Figure 1). This is located close to the Osor River and a local road, 400 m east of the plant, occupying an area of approximately 3150 m^2 and containing 60,000 m^3 of homogeneous-looking material. The particle-size of the tailing material is less than 200 μm ; 80% of this material is smaller than 70 μm .

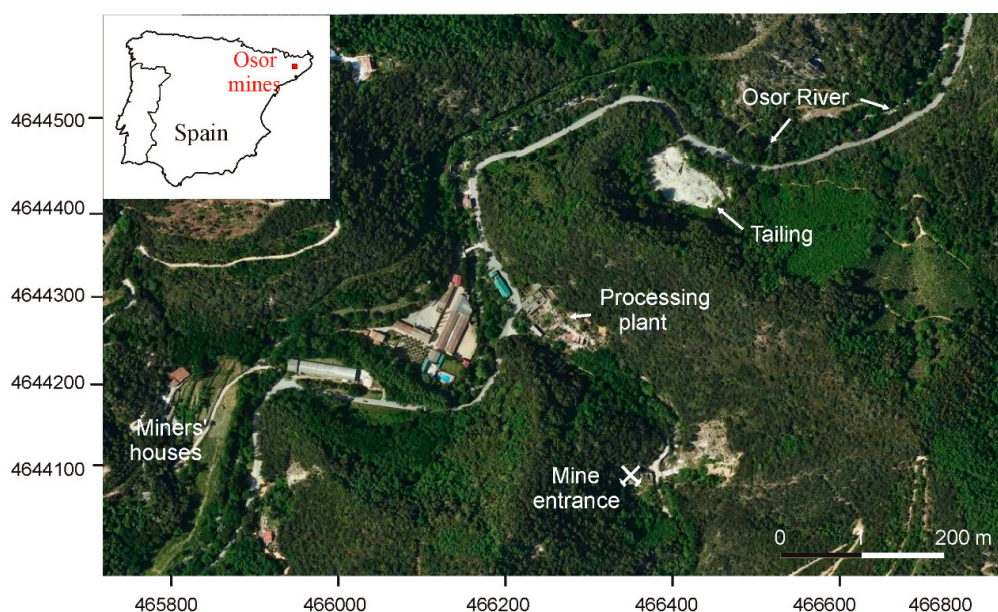


Figure 1. Satellite image showing UTM coordinates and the location of the Osor tailings.

Three composite samples of about 10 kg each were collected from profiles along different levels of height of the tailing. Samples OS-1 and OS-3 represent the lower and uppermost parts of the tailing and OS-2 was obtained at the intermediate height of the tailing. Samples were dried, sieved and quartered to determine their chemical and mineralogical compositions.

Sample OS-2 was selected for experiments because it represents most of the tailing material. This material was powdered and quartered to obtain homogeneous samples. According to the chemical composition of the raw tailing, two glasses were prepared, taking into account that the composition should be equilibrated with respect to the content of former, stabilizer, and refining oxides to produce a commercial quality glass [17]. To this end, the tailing sample was mixed with Na_2CO_3 (PANREAC, Barcelona, Spain cod.131648). Two glasses were obtained in order to establish their industrial behaviour by using 80 wt.% tailing and 20 wt.% Na_2CO_3 (sample G₉₀₋₁₀), and 90 wt.% tailing and 10 wt.% Na_2CO_3 (sample G₈₀₋₂₀). In order to obtain a homogeneous sample, each mixture was homogenized in a ball mill for 48 h.

2.2. Analytical Methods

The particle size distribution of the tailing samples was determined by means of an LS 13 320. Coulter particle size analyser (Beckman, Brea, CA, USA). The chemical composition of tailing samples was determined by X-ray fluorescence (XRF) using a Thermo Scientific ARL ADVANT'XP series instrument (ThermoFisher Scientific, Waltan, MA, USA). The mineralogical composition of the tailings and the phases formed during the thermal treatment of the glasses were determined by X-ray powder diffraction (XRD) using a Bragg-Brentano PANAnalyticalX'Pert Diffractometer. The system has graphite monochromator, an automatic gap, Cu $K\alpha$ -radiation at $\lambda = 1.54061 \text{ \AA}$, powered at 45 kV-40 mA, a scanning range of 4–100° with a 0.017° 2 θ step scan and a 50 s measuring time. Identification and semiquantitative evaluation of the phases was performed by using PANanalytical X'Pert HighScore software (Malvern PANanalytical, Malvern, UK). XRD and scanning electron microscopy (SEM) were used to demonstrate the amorphous structure of the glasses. The equipment used was a compact Phenom XL Desktop SEM (ThermoFisher Scientific, Waltan, MA, USA).

The density of the glass was measured by the Archimedes method using toluene as the immersion liquid following the Spanish standard UNE-EN 993-2:1996 [30].

Thermal analysis of samples was obtained by simultaneous differential thermal analysis and thermogravimetry (DTA-TG), using a Netzsch instrument (STA 409C model NETZSCH-Gerätebau

GmbH, Selb, Bavaria, Germany). Analyses were carried out in the temperature range 25–1300 °C under an air atmosphere, at a constant flow rate of 80 mL/min, in a platinum crucible and at a heating rate of 10 °C/min. The amount of sample analysed was ~75 mg. The aluminium oxide Perkin Elmer 0419–0197 was taken as reference.

Glass transition temperature analysis (T_g), the dilatometric softening point (T_d) and the expansion coefficient were measured with a Linseis horizontal dilatometer L76/1550 (Linseis Messgeräte GmbH, Selb, Bavaria, Germany) using a 2 cm annealing bar. The experiment was carried out from room temperature to 1300 °C at a heating rate of 10 °C/min. Viscosity at T_g had a constant value, independent of composition, of 1012.3 Pa·s [31].

The experimental viscosity–temperature curves (η – T) were drawn using the fixed points defined by Scholze [32] for hot-stage microscopy (HSM) according to rule DIN 51730 [33] and T_g (obtained with dilatometry). In this case, a quenching glass sample, with 3-mm-high test cylinders, was conformed with raw materials powdered under 45 μ m and bound using a 1/20 solution of Elvacite® in acetone, and conformed in a uniaxial press. Test cylinders were heated at a 5 °C/min rate from room temperature to 1500 °C in an air atmosphere. This process was recorded in pictures with ProgRes Capture Pro software (Jenoptik AG, Jena, Germany). Analysis was performed with Hot-Stage software, developed by the Departament de Llenguatges i Sistemes Informàtics, ETSEIB, UPC [34]. The output points were plotted in a graph and then fitted to the Vögel-Fulcher-Tammann (VFT) equation. The theoretical viscosity–temperature curves were obtained using the model defined by Fluegel [35].

Glass colour was measured with a Spectrophotometer CM-700d Konica-Minolta Investment Ltd. (Sensing Business Division, Shanghai, China) and calibrated according to international standards [36]. The spectrophotometer was fitted with a barium sulphate-coated integrating sphere, and a standard illuminant C was used as a light source. The description of the colour was based on three parameters: lightness, saturation and intensity [37], which were based on the use of three coordinates, L^* , a^* and b^* . L^* indicates lightness, 100 being white colour and 0 black. The variables a^* and b^* are the chromatic coordinates: $+a^*$ is the red axis, $-a^*$ is the green axis, $+b^*$ is the yellow axis and $-b^*$ is the blue axis. Low L^* values indicate that the glasses are dark and the a^* and b^* parameters correspond to yellowish green glasses. The colour purity was measured by the Chroma (C) parameter, which is defined by the equation:

$$C^* = \sqrt{a^{*2} + b^{*2}} \quad (1)$$

The intensity of colour is defined by the hue angle (h), which can be determined by Equation (2). Measurement range is 360°, counted clockwise from 0° for the red colour (a^*).

$$h^* = \arctg \frac{b^*}{a^*} \quad (2)$$

The refractive index was obtained using a Shibuya MC-601 refractometer (Shibuya Kogyo CO., Ltd., Tokyo, Japan).

The chemical stability of the glasses was determined by leaching tests in an acidic solution according to the DIN38414-S4 standard [38]. Leachates were analysed using inductively coupled plasma optical emission spectrometry (ICP–OES, Optima 3100, PerkinElmer, Waltham, MA, USA) and ICP–mass spectrometry (ICP–MS, Elan 6000, PerkinElmer, Waltham, MA, USA).

2.3. Glass Production

The raw mixtures were introduced in an alumina-mullite crucible and heated using a globular alumina furnace equipped with molybdenum disilicide Super Kanthal® and a Eurotherm® 902 programmer. Heating started at 2 °C min^{−1} up to 800 °C, followed by a holding time of 2 h, and a second step of heating at 1 °C min^{−1} up to 900 °C, in order to control the Na₂CO₃ decomposition, and a rate of 2 °C min^{−1} up to 1450 °C, where it remained for 4 h. After this, the components were molten. Part of this melt was cast into a metallic mould preheated at 350 °C and annealed near the

glass transition temperature (T_g) at 450 °C for 30 min, followed by free cooling inside the kiln until room temperature was reached. Another part of the melt was quenched via casting on a Cu plate.

3. Results and Discussion

3.1. Characterization of the Tailing Materials

The chemical composition of tailing materials from Osor has small variations, as shown in the analyses of the three samples from different heights of the tailing (Table 1). The differences were not important for preventing their use in a glass-making plant, but the composition needs to be periodically controlled to adjust the additives. The more significant variation was in the SiO_2 content, which varied from 61.76 to 66.11 wt.%. The high calcium content of the tailings, about 12 wt.%, rendered the addition of this component unnecessary. However, the low content in alkaline oxides, 1.33–1.54 wt.% of Na_2O and 2.46–2.66 wt.% of K_2O , rendered the addition of them necessary.

Table 1. Chemical composition, in wt.%, of the raw Osor tailings.

Samples	Os-1	Os-2	Os-3
SiO_2	66.11	61.76	65.69
Al_2O_3	11.69	11.11	11.09
TiO_2	0.42	0.38	0.39
Fe_2O_3	2.85	2.79	2.76
CaO	12.07	12.15	11.31
MgO	1.05	1.03	1.00
BaO	0.50	0.45	0.61
MnO	0.12	0.10	0.11
Na_2O	1.43	1.54	1.33
K_2O	2.66	2.46	2.52
P_2O_5	0.09	0.10	0.11
Zn	0.02	0.61	0.02
Pb	0.33	0.45	0.34
S	0.22	0.48	0.29
F^-		3.70	2.03
$-\text{O} = \text{F}_2$		−1.56	−0.85
Σ	99.59	98.51	98.74

The content of potentially toxic elements was significant; the experimental sample had As 12.6, Bi 0.212, Sb 3.1, Hg 0.064, Cr 35.5, Pb 4930, Zn 4500 and Cu 264 ppm.

The mineralogical composition of the Osor tailing showed small variations in different areas. The most abundant minerals were quartz, albite, K-feldspar, muscovite, chlorite and calcite (Figure 2). Locally, gypsum and sphalerite occurred in relatively significant amounts (Table 2).

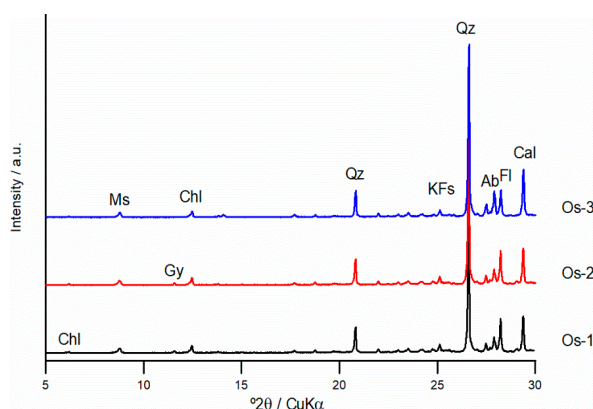


Figure 2. X-ray diffraction patterns of the Osor tailing. Qz: quartz, Kfs: K-feldspar, Pl: plagioclase, Ms: muscovite, Chl: chlorite, Cal: calcite, Fl: fluorite, Gy: gypsum.

Table 2. Semiquantitative mineralogical composition of the Osor tailings in wt.%. Mineral acronyms are the same as those used in Figure 2 (Sp: sphalerite).

Sample	Qz	Kfs	Ab	Ms	Chl	Cal	Fl	Gy	Sp
Os-1	44	5	13	22	5	11	0	0	0
Os-2	40	4	12	19	6	8	8	2.5	0.5
Os-3	39	6	16	19	5	10	5	0	0

3.2. Characterization of Glasses

The XRD diagrams (Figure 3a) show no peaks, indicating the amorphous structure of the glasses produced. The absence of crystalline phases was also tested by SEM observations, which show uniform composition (Figure 3b,c).

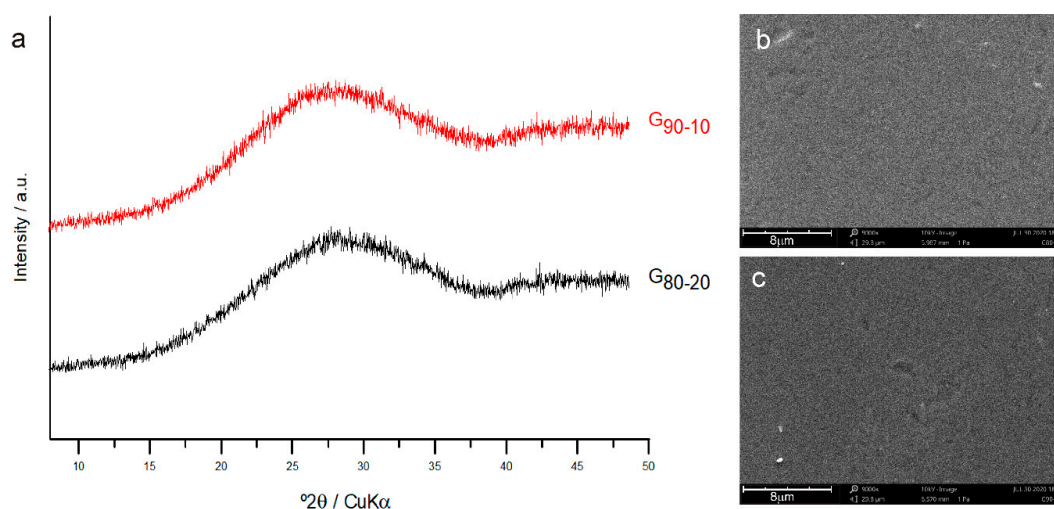


Figure 3. (a) X-ray diffraction patterns for the synthesized glasses, (b) SEM image of glass G₉₀₋₁₀, (c) SEM image of glass G₈₀₋₂₀.

In both the glasses produced (Table 3), only the Na₂O content varied: 7.55 wt.% in the glass made with 90 wt.% of tailing and 14.1 wt.% Na₂O in that made with 80% of tailing. When the Al/Na and 2Al/Ca ratios are ≤1, Al plays a role of former element and is located in a tetrahedral site [39]. In the glasses produced, Al/Na was 0.52 and 0.27, and 2Al/Ca was 0.69. In this case, at least part of the alkaline and alkaline earth elements acted as charge compensators [23]. This composition is suitable for producing durable glass and also for obtaining glass-ceramics; thus, the SiO₂ + Al₂O₃ content was between 60 and 70 wt.% [40]. On the other hand, the high fluorine content made it possible to reach a melting state at a moderate temperature.

Table 3. Chemical composition of the two glasses made with different waste ratios, in wt.%.

Samples	SiO ₂	Al ₂ O ₃	TiO ₂	Fe ₂ O ₃	P ₂ O ₅	ZnO	PbO
G ₉₀₋₁₀	58.22	10.47	0.36	2.63	0.10	0.48	0.40
G ₈₀₋₂₀	54.10	9.73	0.33	2.40	0.10	0.45	0.37
	CaO	MgO	BaO	MnO	Na ₂ O	K ₂ O	F ⁻
G ₉₀₋₁₀	11.45	0.97	0.42	0.89	7.55	2.32	3.49
G ₈₀₋₂₀	10.64	0.90	0.39	0.82	14.10	2.15	3.24

The density values of the produced glasses were 2.54 g/cm³ for the G₈₀₋₂₀ glass and 2.61 g/cm³ for the G₉₀₋₁₀ glass, which are slightly higher values than those of a soda-lime glass (2.44 g/cm³).

3.3. Thermal Behaviour

The DTA of the two samples show glass-transition temperatures (T_g) of 670 and 660 °C for G₈₀₋₂₀ and G₉₀₋₁₀, respectively (Figure 4). The exothermic peak corresponds to the formation of crystalline phases. This event occurred at a slightly lower temperature, 875 °C, and was more pronounced in the G₈₀₋₂₀ glass, whereas in the G₉₀₋₁₀ glass it occurred at 901 °C. Two endothermic peaks correspond to the melting temperature (T_m) of the two crystalline phases formed during the thermal treatment of the glasses. T_m was differed considerably for the glasses: 1066 and 1096 °C in the G₉₀₋₁₀ glass and 1215 and 1220 °C in the G₈₀₋₂₀ glass.

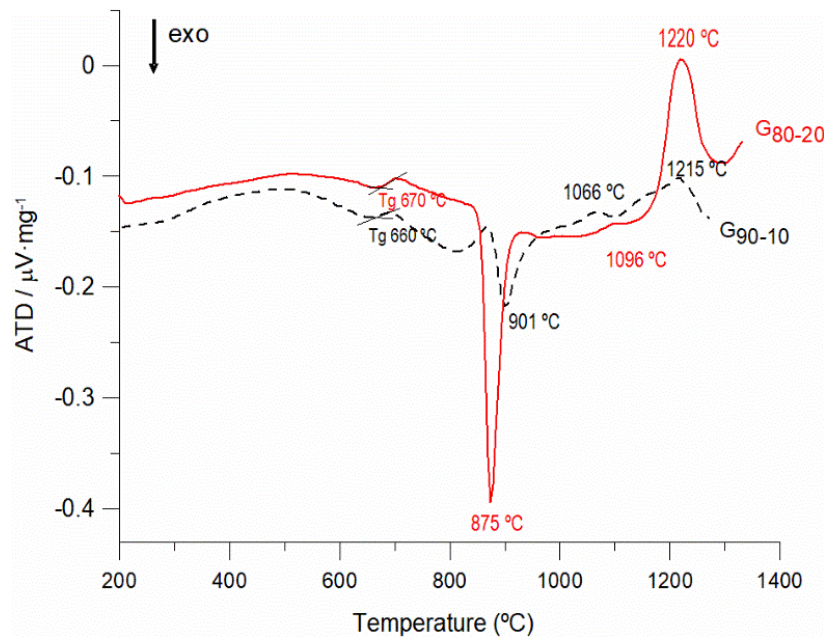


Figure 4. DTA curves of glasses produced from the Osor tailings.

The Hrubý coefficient, Hr , [41] provides a useful criterion to evaluate the stability of glasses [42]. This coefficient is defined by Equation (3):

$$Hr = \frac{T_c - T_g}{T_m - T_c} \quad (3)$$

where T_c is the crystallization temperature, T_g is the glass transition temperature determined by the DTA, T_c is the main temperature of crystallization and T_m is the beginning of the melting. Hr inversely correlates with the tendency to crystallize the glass. The Hr of the G₉₀₋₁₀ and G₈₀₋₂₀ glasses is 1.35 and 0.85, respectively, which is indicative of high stability with respect to crystallization, especially in the glass obtained with 90 wt.% of tailing.

The stability of glasses is important when they contain potentially toxic elements that must be immobilized. Thus, poor stability may lead to the formation of crystals either during annealing of the glass, or afterwards, and lead to cracking of the glass, which increases the leaching rates in such glasses [43]. The higher soda content of the G₈₀₋₂₀ glass significantly decreases working temperatures (forming, conditioning and melting).

The crystalline phases formed during the crystallization of glasses at 1000 °C were different in both glasses, as suspected by the difference between their T_c , which was determined from the DTA (Figure 5).

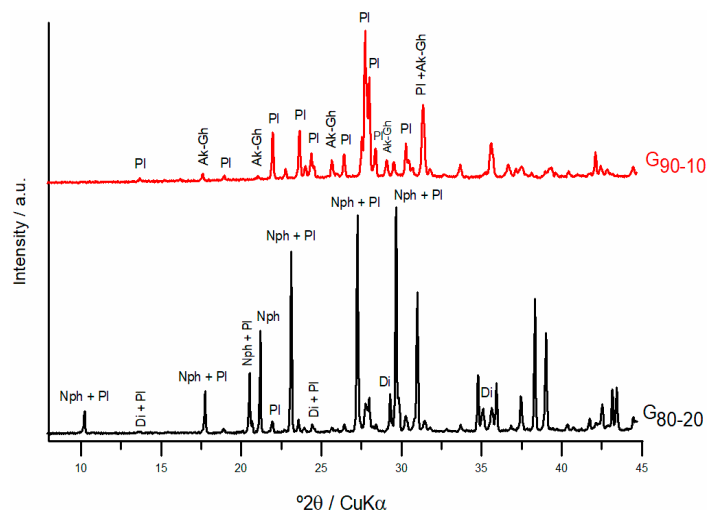


Figure 5. XRD pattern of the Osor glass treated at 1000 °C.

The G₉₀₋₁₀ glass crystallized at higher temperature and the phases formed were richer in Ca, being 88 wt.% of intermediate plagioclase and 12 wt.% of crystals from the akermanite–gehlenite (Ca₂Al(AlSiO₇)–Ca₂Mg(Si₂O₇)) solid solution. In the G₈₀₋₂₀ glass, crystalline phases were 66 wt.% nepheline, 25 wt.% plagioclase and 9 wt.% diopside. The type of plagioclase formed depends on the Ca/Na ratio; with a high content of Na, the crystallization of an intermediate or a Na-rich plagioclase is expected. Therefore, this occurred at a lower temperature than in the Ca-predominant composition, where plagioclase with a composition near the anorthite end member of the plagioclase solid solution (NaCaAlSi₃O₈–Ca₂Al₂Si₂O₈) crystallized.

3.4. Rheological Properties

The dilatometric analysis of the two glasses (Figure 6) yielded a T_g of 637 °C in the G₈₀₋₂₀ glass and 628 °C in the G₉₀₋₁₀ glass. The comparison of these values with those obtained by DTA-TG shows a difference of about 30 °C between both.

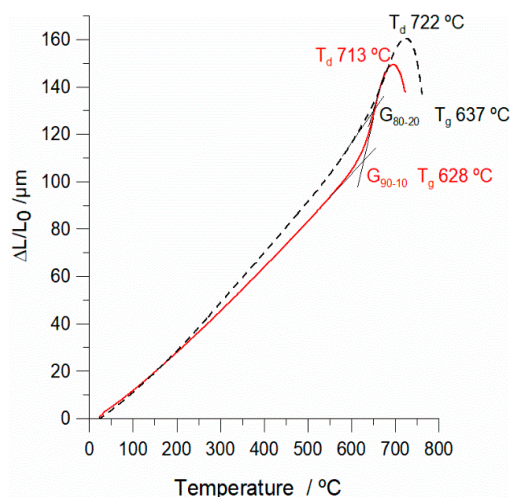


Figure 6. Thermal expansion plot as a function of temperature used to determine T_g and T_d .

The dilatometric softening point, T_d , was 713 and 722 °C (Figure 6), and the calculated thermal expansion coefficient, in the range 25–450 °C, was 10.84×10^{-6} and $9.00 \times 10^{-6} \text{ °C}^{-1}$ for G₈₀₋₂₀ and G₉₀₋₁₀, respectively (Table 6). These values are similar to those of other glasses produced from waste materials, such as slags [44].

Both rheological properties described above were slightly higher in the Osor glasses than in a typical soda-lime glasses. These commercial glasses have a T_g from 550 to 580 °C and an expansion coefficient between 8×10^{-6} and $9.00 \times 10^{-6} \text{ } ^\circ\text{C}^{-1}$ [45].

Viscosity is an important property of the raw glass melt for glass making. The control of this parameter is essential in commercial production for achieving a high efficiency and quality of products [46]. The experimental fixed viscosity points obtained by the automatic image analysis provided by HSM are given in Table 4. Figure 7 shows the images corresponding to the thermal geometrical evolution of the G₈₀₋₂₀ glass.

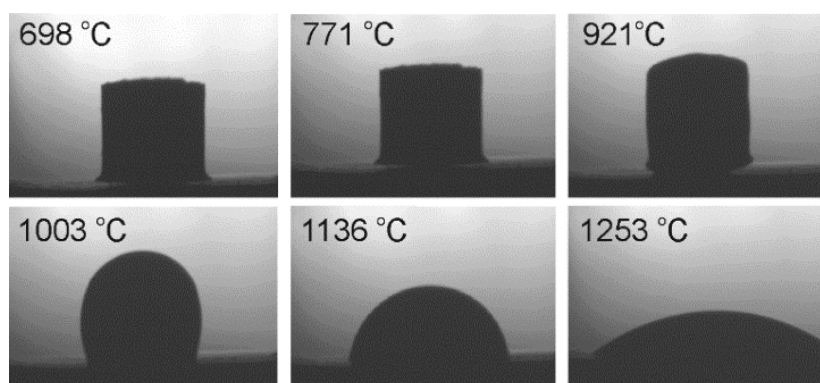


Figure 7. Hot-stage photomicrographs of the G₈₀₋₂₀ glass with the temperatures of fixed viscosity points: first shrinkage, maximum shrinkage, softening, ball, half ball and flow.

According to the working range, glasses can be classified as short glasses and long glasses. The working range of the temperature has been established on viscosity values between 10^6 and $10^3 \text{ Pa}\cdot\text{s}$ [46] or between 10^4 and $10^8 \text{ Pa}\cdot\text{s}$ [47]. Long glasses present a working range of than 400 °C [47]. The forming and shaping of long glasses is easier and allows for working at lower temperatures, while the short glasses become rigid more quickly, enabling automatized production processes [47,48]. The viscosity range between 10^6 and $10^3 \text{ Pa}\cdot\text{s}$ in the case of G₉₀₋₁₀ was 293 °C and in G₈₀₋₂₀ was 479 °C. Therefore, the manufacture of glasses can only be carried out automatically in the case of raw tailing with a higher soda addition.

Table 4. Experimental temperatures for the fixed viscosity points [33,49] and workability calculated temperatures.

Viscosity/Pa·s	Temperature of Fixed Viscosity Points/°C	
	G ₉₀₋₁₀	G ₈₀₋₂₀
Glass transition point ^a /10 ^{12.3}	628	637
First shrinkage/10 ⁹	782	698
Maximum shrinkage/10 ^{7.2}	925	771
Softening 10 ^{5.1}	1025	921
Ball 10 ^{4.4}	1092	1003
Half ball 10 ^{3.6}	1240	1136
Flow 10 ^{3.1}	1270	1253
Calculated temperatures of the significant production viscosities ^b		
Lower annealing point/10 ^{13.5}	620	585
Upper annealing point/10 ¹²	641	641
Forming range/10 ⁸ –10 ³	735–1318	840–1282
Glass condition range/10 ³ –10 ²	1318–1583	1282–1420
Melting range/10 ² –10 ¹	>1583	>1420
Workability interval/10 ⁵ –10 ²	1130–1583	1066–1420

^a Engels and Link [31] included the glass transition point by dilatometer. ^b Calculated using the model by Fluegel [35].

The viscosity-temperature curves for the glasses produced (Figure 8) were obtained using HSM results and by determining the correlation between the fixed points of the known viscosity, the T_g obtained by a dilatometer corresponding to a viscosity of $10^{12.3}$ Pa·s and the Vogel-Fulcher-Tammann (VFT) equation [32]. The G_{80-20} curve has a relatively low fitting in the intermediate region of viscosity, which can be attributed to the crystallization stage [50].

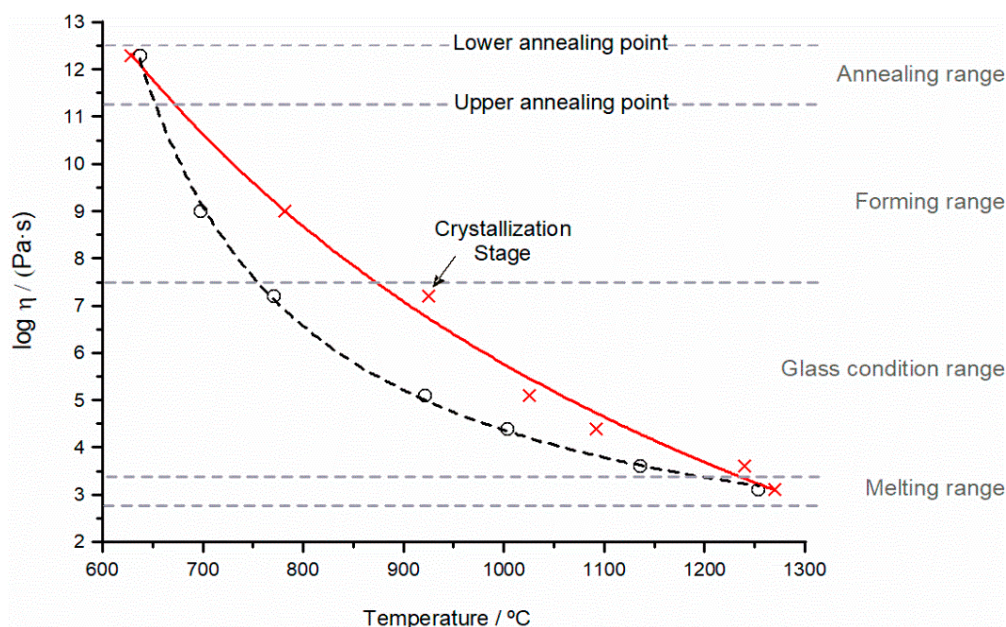


Figure 8. Viscosity–temperature curves and workability intervals of the glasses studied using fixed viscosity points. G_{90-10} = dashed black line (R-squared = 0.9991, Vogel-Fulcher-Tammann (VFT) equation and G_{80-20} = red line (R-squared = 0.9921, VFT).

3.5. Optical Properties

The CIEL AB space [36] provides an objective measure of the colour. In Table 5, the colour parameters for the glasses from the Osor tailings are shown. The low values of C^* indicate that the glasses plotted near the centre of the colour sphere and thus, present low purity. Hue values of the Osor glasses were 93.18 and 110.32°; values between 90 and 180° indicate yellow-green tonality. In Figure 9, these parameters are shown together with others obtained from glasses produced using tailings from different origins, whose characteristics were previously published [13,19,51]. Comparison of the colour parameters from these glasses indicates that tailing glasses usually show medium or dark colour and a low purity. These results are due to the abundant metals content, or the chromophore elements, which usually occurs in tailings from metallic deposits. Yellow-green glasses are common when tailings contain high iron levels and low Mn/Fe ratios [52].

Table 5. Colour parameters for glasses synthesized from tailings.

Glass Type	L^*	a^*	b^*	C^*	h^*
G_{90-10}	45.83	−0.10	0.27	0.29	110.32°
G_{80-20}	44.23	−0.03	0.54	0.54	93.18°

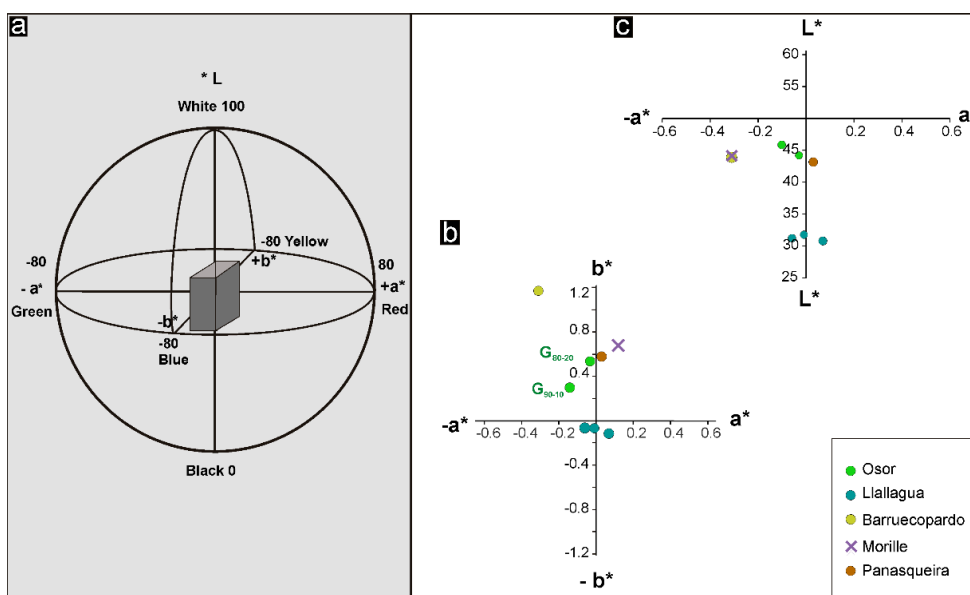


Figure 9. CIE LAB chromatic diagram of the Osor glasses. Data of Llallagua glass from [51]. (a) CIE LAB colour sphere, (b) a^* , b^* colour coordinates, (c) L^* , a^* coordiunates.

The refractive index, n , of both glasses produced was 1.54, which is similar than that of typical soda-lime-silica commercial glasses, with an n of 1.51 to 1.52, and slightly higher than in vitreous glasses because cations fill the interstices in the network [45].

3.6. Leaching Behaviour

The test for leachability of potentially toxic elements from the glasses of the Osor tailings, determined using the DIN 38414-S4 standard [36], showed that the concentrations of metals in the leachates were always under the threshold limits established in the standard [36]. These results suggest that the metals were fixed in the structure of the glasses. Metal retention was similar in both glasses, although the G_{80-10} glasses better retained metals. The Pb content in the G_{90-10} glass was 4437 ppm, from this, 0.230 ppm was removed during the leaching test, which represents 0.0005 wt.% of the total amount of Pb in this glass (Table 6). These results indicate the high stability of the toxic elements in the glassy structure, as has been reported in other glasses made from tailings [13,19,51] and in industrial waste products [53].

Table 6. Chemical composition of glasses, their leachates and threshold limits (TL) according to the DIN 38414-S4 standard. Results are expressed in ppm.

Material	Sample	Cu	Zn	Pb	As	Cr	Ni	Cd	Hg
Glass	G_{90-10}	238	4.050	4.437	10.85	31.95	17.10	11.88	57.60
Glass	G_{80-20}	211	3.600	3.944	9.65	28.40	15.20	10.56	51.20
Leachate	G_{90-10}	0.098	0.231	0.230	0.008	0.017	0.076	0.001	0.001
Leachate	G_{80-20}	0.079	0.244	0.060	0.006	0.013	0.020	0.001	0.002
	TL	2.00	4.00	0.50	0.50	0.50	0.40	0.04	0.01
Wt.% leachate									
Glass	G_{90-10}	0.004	0.001	0.0005	0.006	0.005	0.040	0.001	0.203
Glass	G_{80-20}	0.003	0.001	0.0001	0.005	0.004	0.012	0.001	0.347

4. Conclusions

Tailings from the Osor mines are rich in calcium and only soda needs to be added to make commercial glass.

Two different doses of Na_2CO_3 were used for the experimental glasses. The transition and melting temperatures were higher in the case glasses with less soda content. The H_r of G_{90-10} was higher than that of G_{80-20} , suggesting that glass with less soda content was more stable with respect to crystallization. However, G_{80-20} displayed a wider range of workability temperatures. Therefore, glasses were more stable, but more difficult to produce in the compositions with 10% Na_2CO_3 compared to those with 20% Na_2O_3 .

The composition of the tailings from the Osor mines is suitable for the manufacture of commercial glass. The glasses obtained from the tailings retain potentially toxic elements in their structure and prevent environmental contamination. Although both compositions retain these potentially toxic elements, glass with 20% Na_2CO_3 is more efficient.

The tailing and Na_2O_3 dosages are suitable for making commercial glass. Although the higher Na_2O_3 content resulted in greater efficiency, the cost of production should also be taken into account before a final decision is made.

Author Contributions: Conceptualization, M.G.-V. and P.A.; methodology, M.G.-V., S.M. and P.A.; software, M.G.-V., O.T. and P.A.; validation, S.M. and M.G.-V.; formal analysis, O.T., P.A. and M.G.-V.; investigation, O.T., N.R. and L.M.D.; resources, M.G.-V. and S.M.; data curation, O.T.; writing—original draft preparation, P.A. and M.G.-V.; writing—review, all authors; visualization, M.G.-V. and P.A.; supervision, M.G.-V., P.A. and S.M.; project administration and funding acquisition, M.G.-V. and P.A. All authors have read and agreed to the published version of the manuscript.

Funding: This study benefitted from the budget granted by the Generalitat de Catalunya (Autonomous Government of Catalonia) to the Consolidated Research Group SGR-2017SGR1687 and 2017SGR0707.

Acknowledgments: The authors thank the staff of the Scientific-Technical Service Unit of the University of Barcelona (CCiTUB) for their technical support.

Conflicts of Interest: The authors declare no conflict of interest.

References

1. Grangeia, C.; Ávila, P.; Matias, M.; Da Silva, E.F. Mine tailings integrated investigations: The case of Rio tailings (Panasqueira Mine, Central Portugal). *Eng. Geol.* **2011**, *123*, 359–372. [[CrossRef](#)]
2. Ritcey, G. *Tailings Management: Problems and Solutions in the Mining Industry*; Elsevier: Amsterdam, The Netherlands, 1989.
3. Dold, B. Evolution of Acid Mine Drainage Formation in Sulphidic Mine Tailings. *Minerals* **2014**, *4*, 621–641. [[CrossRef](#)]
4. Chen, T.; Yan, Z.A.; Xu, D.; Wang, M.; Huang, J.; Yan, B.; Xiao, X.; Ning, X. Current situation and forecast of environmental risks of a typical lead-zinc sulfide tailings impoundment based on its geochemical characteristics. *J. Environ. Sci.* **2020**, *93*, 120–128. [[CrossRef](#)] [[PubMed](#)]
5. Jamieson, H.E.; Walker, S.R.; Parsons, M.B. Mineralogical characterization of mine waste. *Appl. Geochem.* **2015**, *57*, 85–105. [[CrossRef](#)]
6. Mudd, G.M.; Boger, D.V. The Ever Growing Case for Paste and Thickened Tailings-towards More Sustainable Mine Waste Management. *J. Aust. Inst. Min. Metall.* **2013**, *2*, 56–59.
7. Schoenberger, E. Environmentally sustainable mining: The case of tailings storage facilities. *Resource. Policy* **2016**, *49*, 119–128. [[CrossRef](#)]
8. Tayebi-Khorami, M.; Edraki, M.; Corder, G.; Golev, A. Re-Thinking Mining Waste through an Integrative Approach Led by Circular Economy Aspirations. *Minerals* **2019**, *9*, 286. [[CrossRef](#)]
9. Lèbre, É.; Corder, G.; Golev, A. The role of the mining industry in a circular economy: A framework for resource management at the mine site level. *J. Ind. Ecol.* **2017**, *21*, 662–672. [[CrossRef](#)]
10. Marabini, A.M.; Plescia, P.; Maccari, D.; Burragato, F.; Pelino, M. New materials from industrial mining wastes: Glass-ceramic and glass and rock-wool fibre. *Int. J. Miner. Process.* **1998**, *53*, 121–134. [[CrossRef](#)]
11. Bingham, P.A.; Hand, R.J.; Forder, S.D.; Lavaysierre, A. Vitrified Metal Finishing Wastes II. Thermal and Structural Characterisation. *J. Hazard. Mater.* **2005**, *122*, 129–138. [[CrossRef](#)] [[PubMed](#)]
12. Park, H.S.; Park, J.H. Vitrification of red mud with mine wastes through melting and granulation process—Preparation of glass ball. *Non-Cryst. Solids* **2017**, *475*, 129–135. [[CrossRef](#)]

13. Alfonso, P.; Tomasa, O.; Garcia-Valles, M.; Tarragó, M.; Martínez, S.; Esteves, H. Potential of tungsten tailings as glass raw materials. *Mater. Lett.* **2018**, *228*, 456–458. [[CrossRef](#)]
14. Okereafor, U.; Makhatha, M.; Mekuto, L.; Mavumengwana, V. Gold Mine Tailings: A Potential Source of Silica Sand for Glass Making. *Minerals* **2020**, *10*, 488. [[CrossRef](#)]
15. Kim, Y.; Kim, M.; Sohn, J.; Park, H. Applicability of gold tailings, waste limestone, red mud, and ferronickel slag for producing glass fibers. *J. Clean. Prod.* **2018**, *203*, 957–965. [[CrossRef](#)]
16. Shao, H.; Liang, K.; Peng, F.; Zhou, F.; Hu, A. Production and properties of cordierite-based glass-ceramics from gold tailings. *Miner. Eng.* **2005**, *18*, 635–637. [[CrossRef](#)]
17. Lay, G.F.T.; Rockwell, M.C.; Wiltshire, J.C.; Ketata, C. Characteristics of silicate glasses derived from vitrification of manganese crust tailings. *Ceram Int.* **2009**, *35*, 1961–1967.
18. Baowei, L.; Leibo, D.; Xuefeng, Z.; Xiaolin, J. Structure and performance of glass–ceramics obtained by Bayan Obo tailing and fly ash. *J. Non-Cryst. Solids* **2013**, *380*, 103–108. [[CrossRef](#)]
19. Alfonso, P.; Castro, D.; García-Vallès, M.; Tarragó, M.; Tomasa, O.; Martínez, S. Recycling of tailings from the Barruecopardo tungsten deposit for the production of glass. *J. Therm. Anal. Calorim.* **2016**, *125*, 681–687. [[CrossRef](#)]
20. Karamanov, A.; Hamzawy, E.M.; Karamanova, E.; Jordanov, N.B.; Darwish, H. Sintered glass-ceramics and foams by metallurgical slag with addition of CaF₂. *Ceram. Int.* **2020**, *46*, 6507–6516. [[CrossRef](#)]
21. Hill, R.; Wood, D.; Thomas, M. Trimethylsilylation analysis of the silicate structure of fluoro-alumino-silicate glasses and the structural role of fluorine. *J. Mater. Sci.* **1999**, *34*, 1767–1774. [[CrossRef](#)]
22. Pei, F.; Zhu, G.; Li, P.; Guo, H.; Yang, P. Effects of CaF₂ on the sintering and crystallisation of CaO–MgO–Al₂O₃–SiO₂ glass-ceramics. *Ceram. Int.* **2020**, *46*, 17825–17835. [[CrossRef](#)]
23. Cormier, L.; Neuville, D.R. Ca and Na environments in Na₂O–CaO–Al₂O₃–SiO₂ glasses: Influence of cation mixing and cation-network interactions. *Chem. Geol.* **2004**, *213*, 103–113. [[CrossRef](#)]
24. Angeli, F.; Gaillard, M.; Jollivet, P.; Charpentier, T. Contribution of ⁴³Ca MAS NMR for probing the structural configuration of calcium in glass. *Chem. Phys. Lett.* **2007**, *440*, 324–328. [[CrossRef](#)]
25. Ligeró, F.B. La minería a Osor. *Quad. Selva* **1995**, *8*, 137.
26. Corcoll, N.; Bonet, B.; Morin, S.; Tlili, A.; Leira, M.; Guasch, H. The effect of metals on photosynthesis processes and diatom metrics of biofilm from a metal-contaminated river: A translocation experiment. *Ecol. Indic.* **2012**, *18*, 620–631. [[CrossRef](#)]
27. Navarro, A.; Font, X.; Viladevall, M. Metal Mobilization and Zinc-Rich Circumneutral Mine Drainage from the Abandoned Mining Area of Osor (Girona, NE Spain). *Mine Water Environ.* **2015**, *34*, 329–342. [[CrossRef](#)]
28. Bori, J.; Vallès, B.; Navarro, A.; Riva, M.C. Ecotoxicological risks of the abandoned F–Ba–Pb–Zn mining area of Osor (Spain). *Environ. Geochem. Health* **2017**, *39*, 665–679. [[CrossRef](#)] [[PubMed](#)]
29. Piqué, À.; Canals, À.; Grandia, F.; Banks, D.A. Mesozoic fluorite veins in NE Spain record regional base metal-rich brine circulation through basin and basement during extensional events. *Chem. Geol.* **2008**, *257*, 139–152. [[CrossRef](#)]
30. UNE-EN 993-2:1996. *Métodos de Ensayo para Productos Refractarios Conformados Densos. Parte 2: Determinación de la Densidad Absoluta. Spanish Standard*; AENOR: Madrid, Spain, 1996.
31. Engels, M.; Link, S. Bubble control in ceramic glazes. *Interceram* **2006**, *3*, 152–156.
32. Scholze, H. Der Einfluss von Viskosität und Oberflächenspannung auf erhitzungsmikroskopische Messungen an Gläsern. *Ber. Dtsch. Keram. Ges.* **1962**, *39*, 63–68.
33. DIN 51730. *Determination of ash Fusion Behaviour, German Standard*; DIN Deutsches Institut für Normung, E.V.: Berlin, Germany, 1976.
34. Garcia-Valles, M.; Hafez, H.; Cruz-Matías, I.; Vergés, E.; Aly, M.H.; Nogués, J.M.; Ayala, D.; Martínez, S. Calculation of viscosity–temperature curves for glass obtained from four wastewater treatment plants in Egypt. *J. Therm. Anal. Calorim.* **2013**, *111*, 107–114. [[CrossRef](#)]
35. Fluegel, A. Glass viscosity calculation based on a global statistical modeling approach. *Glass Technol.* **2007**, *48*, 13–30.
36. CIE. *Technical Report, Colorimetry*; Commission Internationale de L’Eclairage: Vienna, Austria, 1931.
37. McGuire, R.G. Reporting of objective color measurements. *HortScience* **1992**, *27*, 1254–1255. [[CrossRef](#)]
38. DIN 38414-S4. *Schlamm und Sedimente, Bestimmung der Eluierbarkeit mit Wasser*; DIN Deutsches Institut für Normung, E.V.: Berlin, Germany, 1984.
39. Mysen, B.O. *Structure and Properties of Silicate Melts*; Elsevier: Amsterdam, The Netherlands, 1988.

40. Barbieri, L.; Lancettotti, I.; Manfredini, T.; Queralto, I.; Rincon, J.M.; Romero, M. Design, obtainment and properties of glasses and glass–ceramics from coal fly ash. *Fuel* **1999**, *78*, 271–276. [[CrossRef](#)]
41. Hrubý, A. Evaluation of glass-forming tendency by means of DTA. *Czechoslov. J. Phys. B* **1972**, *22*, 1187–1193. [[CrossRef](#)]
42. Kozmidis-Petrovic, A.; Šesták, J. Forty years of the Hrubý glass-forming coefficient via DTA when comparing other criteria in relation to the glass stability and vitrification ability. *J. Therm. Anal. Calorim.* **2012**, *110*, 997–1004. [[CrossRef](#)]
43. Donald, I.W.; Metcalfe, B.L.; Taylor, R.J. The immobilization of high level radioactive wastes using ceramics and glasses. *J. Mater. Sci.* **1997**, *32*, 5851–5887. [[CrossRef](#)]
44. Wu, J.P.; Rawlings, R.D.; Boccaccini, A.R. A glass–ceramic derived from high TiO₂-containing slag: Microstructural development and mechanical behaviour. *J. Am. Ceram. Soc.* **2006**, *89*, 2426–2433. [[CrossRef](#)]
45. Shelby, J.E. *Introduction to Glass Science and Technology*; Royal Society of Chemistry: Cambridge, UK, 2005.
46. Cheng, J.; Xiao, Z.; Yang, K.; Wu, H. Viscosity, fragility and structure of Na₂O–CaO–Al₂O₃–SiO₂ glasses of increasing Al/Si ratio. *Ceram. Int.* **2013**, *39*, 4055–4062. [[CrossRef](#)]
47. Fernández Navarro, J.M. *La Sociedad Española de Cerámica y Vidrio a lo Largo de Medio Siglo*; Sociedad Española de Cerámica y Vidrio: Madrid, Spain, 1991.
48. Karamanov, A.; Di Gioacchino, R.; Piscicella, P.; Pelino, M.; Hreglich, A. Viscosity of iron rich glasses obtained from industrial wastes. *Glass Technol.* **2002**, *43*, 34–38.
49. Pascual, M.J.; Pascual, L.; Duran, A. Determination of the viscosity-temperature curve for glasses on the basis of fixed viscosity-temperature determined by hot stage microscopy. *Phys. Chem. Glasses* **2001**, *42*, 61–66.
50. Khalil, T.K.; Boccaccini, A.R. Heating microscopy study of the sintering behaviour of glass powder compacts in the binary system SiO₂–TiO₂. *Mater. Lett.* **2002**, *56*, 317–321. [[CrossRef](#)]
51. Arancibia, J.R.H.; Alfonso, P.; Garcia Vallès, M.; Martínez Manent, S.; Parcerisa, D.; Canet, C.; Romero, F.M. Manufacturing of glass from tin mining tailings in Bolivia. *Bol. Soc. Esp. Ceram. Vidr.* **2013**, *52*, 143–150. [[CrossRef](#)]
52. Mirti, P.; Davit, P.; Gulmini, M. Colourants and opacifiers in seventh and eighth century glass investigated by spectroscopic techniques. *Anal. Bioanal. Chem.* **2002**, *372*, 221–229. [[CrossRef](#)]
53. Piscicella, P.; Crisucci, S.; Karamanov, A.; Pelino, M. Chemical durability of glasses obtained by vitrification of industrial wastes. *Waste Manag.* **2001**, *21*, 1–9. [[CrossRef](#)]



© 2020 by the authors. Licensee MDPI, Basel, Switzerland. This article is an open access article distributed under the terms and conditions of the Creative Commons Attribution (CC BY) license (<http://creativecommons.org/licenses/by/4.0/>).